

## How Sugars Protect Dry Protein Structure

Julia A. Brom, Ruta G. Petrikis, and Gary J. Pielak\*

Cite This: *Biochemistry* 2023, 62, 1044–1052

Read Online

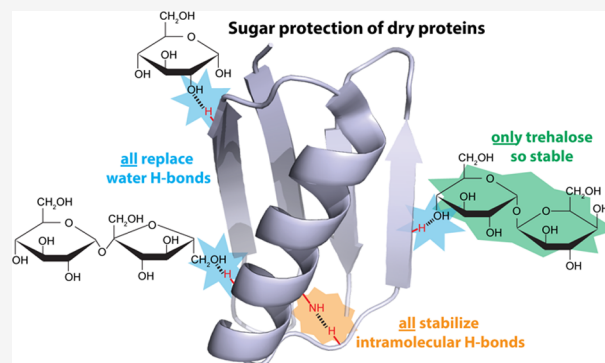
ACCESS |

Metrics &amp; More

Article Recommendations

Supporting Information

**ABSTRACT:** Extremotolerant organisms and industry exploit sugars as desiccation protectants, with trehalose being widely used by both. How sugars, in general, and the hydrolytically stable sugar trehalose, in particular, protect proteins is poorly understood, which hinders the rational design of new excipients and implementation of novel formulations for preserving lifesaving protein drugs and industrial enzymes. We employed liquid-observed vapor exchange nuclear magnetic resonance (LOVE NMR), differential scanning calorimetry (DSC), and thermal gravimetric analysis (TGA) to show how trehalose and other sugars protect two model proteins: the B1 domain of streptococcal protein G (GB1) and truncated barley chymotrypsin inhibitor 2 (CI2). Residues with intramolecular H-bonds are most protected. The LOVE NMR and DSC data indicate that vitrification may be protective. Combining LOVE NMR and TGA data shows that water retention is not important. Our data suggest that sugars protect protein structure as they dry by strengthening intraprotein H-bonds and water replacement and that trehalose is the stress-tolerance sugar of choice because of its covalent stability.



### INTRODUCTION

Protein-based drugs are among the most precise and powerful therapeutics, yet their instability in solution and the high cost of transport and storage hinder their availability.<sup>1–5</sup> Drying extends shelf lives and permits storage at ambient temperature, but most proteins do not survive desiccation, so protective molecules called excipients are added to protect proteins from desiccation stress.<sup>6–9</sup> Excipients may be other proteins, polymers, osmolytes, or sugars.<sup>9,10</sup> Among sugar excipients, trehalose is notable because it is widely used as a desiccation protectant by both biology and industry.<sup>11–15</sup> Trehalose protects proteins both in solution<sup>16</sup> and in the dry state.<sup>17,18</sup>

The mechanism of trehalose protection, and sugar protection in general, is unknown, but there are several ideas: water replacement, water retention, and vitrification.<sup>5,19,20</sup> In water replacement, sugars substitute stabilizing hydrogen bonds that water provides to the protein in solution. This idea is supported by Fourier transform infrared spectroscopy data on dry proteins in sugars.<sup>5,21,22</sup> For water retention, sugars trap a protective layer of water on the surface of dry proteins. A solution-based neutron diffraction study on N-methyl acetamide with trehalose supports this view.<sup>23</sup> Vitrification posits that the glassy, amorphous sugar matrix formed upon drying immobilizes proteins below the glass-transition temperature ( $T_g$ ) of the matrix, preventing unfolding and degradation by limiting mobility.<sup>5</sup> Protection of alkaline phosphatase activity is  $T_g$ -dependent near  $T_g$  supporting this idea.<sup>24</sup>

We developed liquid-observed vapor exchange (LOVE) NMR to discriminate hypotheses and bring new mechanisms to light. LOVE NMR provides unique, residue-level insight into dry protein structure and protection.<sup>17,25,26</sup> The technique uses solution NMR to quantify the extent of hydrogen–deuterium exchange between  $D_2O$  vapor and amide protons of a dried protein. Since amide protons are less likely to exchange with deuterons if occluded or involved in intra- or intermolecular H-bonds,<sup>27–29</sup> the amide–proton signal remaining after vapor exchange is proportional to the fraction of the dry protein population for which a given residue is protected against exchange.<sup>17</sup> Maintenance of native structure upon dehydration correlates with functional recovery after rehydration,<sup>21</sup> so this measurement is relevant to overall protection.<sup>21</sup> In summary, LOVE NMR reveals excipient effects on dry protein structure at the residue level.

Here, we use LOVE NMR, differential scanning calorimetry (DSC), and thermal gravimetric analysis (TGA) to understand how sugars protect two model proteins, the B1 domain of streptococcal protein G (GB1) and truncated barley chymotrypsin inhibitor 2 (CI2). GB1 is a 56-residue protein with 11 residues that are only available for hydrogen–

Received: December 9, 2022

Revised: January 27, 2023

Published: February 18, 2023



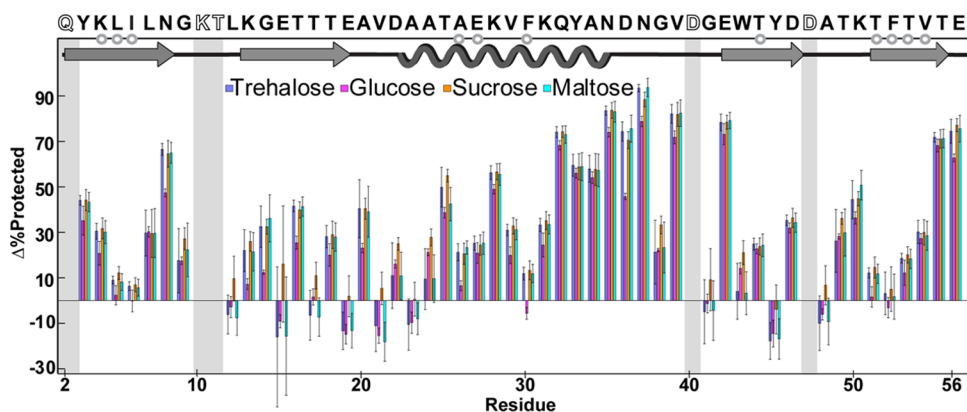


**Figure 1.** Change in dry-state protection of GB1 upon freeze-drying in trehalose, glucose, sucrose, or maltose.  $\Delta\%\text{Protected} = \%\text{Protected}_{+\text{sugar}} - \%\text{Protected}_{-\text{sugar}}$ . The primary and secondary structure of GB1 (PDB 2QMT) is shown at the top. Gray circles indicate solution global-unfolding residues. Shaded boxes and open letters indicate missing data from rapid back exchange. Error bars represent standard deviations propagated from triplicate analysis.

deuterium exchange when the protein is completely unfolded (“global-unfolding residues”);<sup>30</sup> CI2 is a 64-residue protein with eight global unfolders.<sup>31</sup> To uncover what makes the nonreducing glucose disaccharide trehalose remarkable, we compared it to glucose, a reducing monosaccharide; sucrose, a nonreducing disaccharide of glucose and fructose; and maltose, a reducing glucose disaccharide (Figure S1). To understand the chemistry of protection, we also examined the effects of two deoxy sugars and two sugar alcohols (Figure S1).

## ■ EXPERIMENTAL DETAILS

**Materials.** Ampicillin, trehalose dihydrate, citric acid monohydrate, fucose, rhamnose, 1,2,3-hexanetriol, L-galactose, citric acid trisodium salt,  $\text{K}_2\text{CO}_3$  (Sigma-Aldrich), maltose monohydrate (Alfa Aesar), glucose (MP Biomedicals, LLC), sucrose (Acros Organics), sorbitol, and HEPES (Fisher Bioreagents) were used without further purification.  $\text{H}_2\text{O}$  with a resistivity  $>17\text{ M}\Omega\text{ cm}^{-1}$  was used to prepare buffers. pH values are direct readings, uncorrected for the deuterium isotope effect.<sup>32</sup>  $^{15}\text{N}$ -enriched GB1 (UniProt P19909) and truncated CI2 (UniProt P01053) were expressed in Agilent BL21 Gold (DE3) *Escherichia coli* in minimal media and purified, characterized, and stored as described.<sup>17,33</sup>

**Liquid-Observed Vapor Exchange (LOVE) NMR.** The LOVE NMR procedure<sup>26</sup> was slightly modified. Samples previously written as “ $T_0$ ” and “ $T_{24}$ ” are now referred to as “ $t_0$ ” and “ $t_{24}$ ” to avoid confusion with temperature. Aliquots were resuspended with or without sugar in 1.5 mM HEPES pH 6.5 and flash-frozen for 3 min in a  $\text{CO}_2$ (s)/ethanol bath before lyophilization for 24 h. Following lyophilization, the  $t_0$  sample was left sealed at room temperature for 24 h, and a saturated solution of  $\text{K}_2\text{CO}_3$  in  $\text{D}_2\text{O}$  was used to maintain 43% relative humidity<sup>34,35</sup> in the chamber where the  $t_{24}$  sample was kept for 24 h. Both samples were then resuspended in 100 mM citrate buffer, pH 4.5, for data acquisition. For back-exchange correction, the  $t_{24}$  sample was left in the spectrometer for  $\sim 6$  h, during which time an additional 9–11 spectra were acquired. All NMR spectra were acquired as described.<sup>26</sup>

**Thermogravimetric Analysis (TGA).** The GB1  $t_0$  and  $t_{24}$  samples alone and in sugars or sugar alcohols were prepared as described above. Samples,  $\sim 0.5$  to 2 mg, were loaded into a TA Instruments model 550 thermogravimetric analyzer on an open Pt pan and heated from 25 to  $\sim 220\text{ }^\circ\text{C}$  at a rate of  $5\text{ }^\circ\text{C}/\text{min}$  under a 60 mL/min  $\text{N}_2(\text{g})$  sample purge with a balance purge

of 40 mL/min. The distinct mass loss ending at  $\sim 125$ – $155\text{ }^\circ\text{C}$  was used to quantify the  $\text{H}_2\text{O}/\text{D}_2\text{O}$  content.<sup>36,37</sup> Thermograms were analyzed using Trios software.

**Differential Scanning Calorimetry (DSC).** The GB1  $t_0$  and  $t_{24}$  samples alone and in sugars or sugar alcohols were prepared as described above. Samples weighing  $\sim 1$  to 3 mg were sealed in Tzero Hermetic Al pans and loaded into a TA Instruments DSC 250 equipped with a TA Instruments Refrigerated Cooling System 90. An identical, empty pan was used as a reference, and the sample cell was purged with 50 mL/min  $\text{N}_2(\text{g})$ . To eliminate differing thermal history effects on the reversible glass transition,<sup>38–42</sup> samples were cooled below their glass-transition temperatures ( $T_g$ ), heated at  $7.5\text{ }^\circ\text{C}/\text{min}$  to above  $T_g$  and then cooled below  $T_g$  where they remained for 1 min. Samples were again heated at  $7.5\text{ }^\circ\text{C}/\text{min}$  past their  $T_g$ ;  $T_g$  was measured from this scan. Thermograms were analyzed using Trios software. The midpoint of the endothermal baseline shift is reported as  $T_g$ .<sup>39,42</sup>

## ■ RESULTS

**Sugars.** We performed LOVE NMR on GB1 and CI2 by themselves and in the presence of trehalose, glucose, sucrose, or maltose. Samples comprised 500  $\mu\text{M}$  ( $\sim 3\text{ g/L}$ ) protein alone or in 20 g/L sugar or sugar alcohol in a total volume of 650  $\mu\text{L}$  ( $\sim 6.7\text{ g sugar/g protein}$ ,  $\sim 250\text{ mol monosaccharide/mol protein}$ ). %Protected values (Tables S1 and S2) of protein dried in buffer alone were subtracted from %Protected values acquired in the sugars to give  $\Delta\%\text{Protected}$  (Figure 1). The pattern for trehalose is higher resolution than our original efforts<sup>17</sup> because the current data were acquired at a lower relative humidity (43 vs 75%) and with a correction for back exchange.<sup>26</sup>

The four sugars provide nearly identical protection (Figures 1, 2, and S2). Drying GB1 in the presence of 20 g/L trehalose, glucose, sucrose, or maltose increases the average %Protected value by  $30 \pm 4$ ,  $24 \pm 4$ ,  $35 \pm 3$ , and  $30 \pm 4\%$ , respectively. Drying CI2 in the presence of 20 g/L trehalose, glucose, or sucrose increases the average %Protected value by  $31 \pm 3$ ,  $29 \pm 4$ , and  $28 \pm 3\%$ , respectively. Uncertainties are the standard error of the mean. The disaccharides outperform glucose on average for GB1, but the data are within the uncertainty of  $\Delta\%\text{Protected}$  values for most residues. Linear regressions of  $\Delta\%\text{Protected}$  in glucose, sucrose, and maltose vs  $\Delta\%\text{Protected}$  in trehalose yield slopes near 1 (between 0.7 and 1.3),

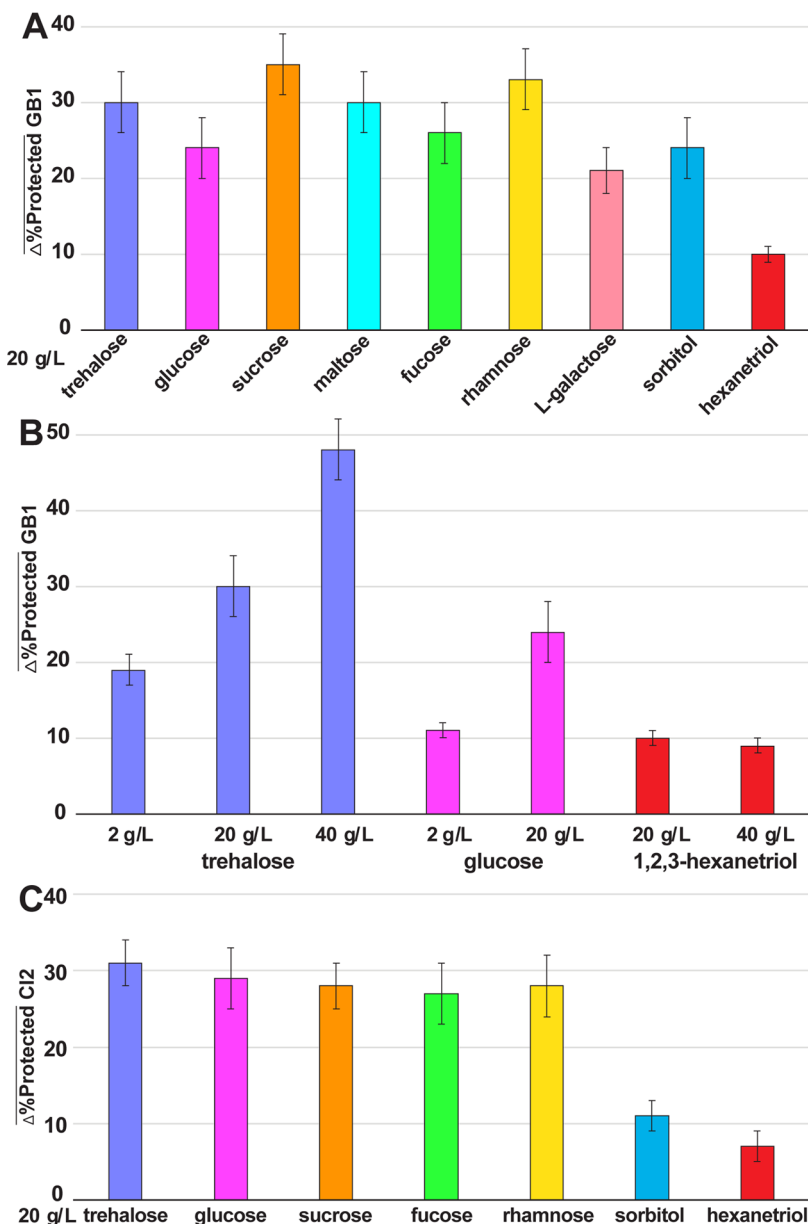


**Figure 2.** Average increase in dry-state protection of GB1 and CI2 upon freeze-drying in sugar or sugar alcohol.  $\Delta\%\text{Protected} = \%\text{Protected}_{+\text{sugar}} - \%\text{Protected}_{-\text{sugar}}$  (A) GB1 in 20 g/L sugar or sugar alcohol. (B) GB1 in varying doses of sugar or sugar alcohols. (C) CI2 in 20 g/L sugar or sugar alcohol. Error bars represent standard error from averaging  $\Delta\%\text{Protected}$  for all residues of GB1 or CI2 after triplicate analysis, except for L-galactose and 40 g/L trehalose, which were analyzed once, and the uncertainty is from triplicated measurements of GB1 alone, assuming the same uncertainty for the differences.

correlation coefficients near 1 (greater than 0.88), and intercepts near 0 (less than 14%; [Figures S3 and S4](#) and [Table S3](#)).

**Deoxy Sugars and Sugar Alcohols.** We performed LOVE NMR on GB1 and CI2 in the presence of two deoxy sugars, fucose (6-deoxy-L-galactose) and rhamnose (6-deoxy-L-mannose), a linear sugar alcohol, sorbitol, and a triply deoxy sugar alcohol, 1,2,3-hexanetriol. We also used L-galactose to compare with fucose. Like the experiments described above, samples comprised 500  $\mu\text{M}$  ( $\sim 3$  g/L) GB1 or CI2 alone or in 20 g/L sugar in a total volume of 650  $\mu\text{L}$ . Unlike other experiments, which were triplicated, L-galactose was assessed only once because the sugar is expensive.

Drying in these deoxy sugars provides similar protection to the non-deoxy sugars ([Figure 2](#) and [Tables S4 and S5](#)). For

GB1, drying in 20 g/L fucose and rhamnose increases the average %Protected compared to the absence of sugar by  $26 \pm 4$  and  $33 \pm 4$ , respectively, and  $27 \pm 4$  and  $28 \pm 4$  for CI2. For GB1, L-galactose increases the average %Protected by  $21 \pm 3\%$ , within the uncertainty of its deoxy counterpart ([Figure 2](#) and [Table S4](#)). Uncertainties are the standard error of the mean. Linear regressions of residue-level  $\Delta\%\text{Protected}$  values in fucose, rhamnose, and L-galactose *vs* those in trehalose yield slopes and correlation coefficients near 1 and intercepts near 0 ([Figures S3 and S4](#) and [Table S3](#)).

Drying in sugar alcohols gives different effects for each protein ([Figure 2](#)). For GB1, drying in 20 g/L sorbitol and 1,2,3-hexanetriol increases the average %Protected compared to the absence of an additive by  $24 \pm 4$  and  $10 \pm 1\%$ , respectively. The values for CI2 are  $11 \pm 2$  and  $7 \pm 4\%$ ,

respectively. Uncertainties are the standard error of the mean. Linearization decreases protection for CI2 but not GB1. Removing three hydroxyl groups decreases protection for both proteins (Figure 2).

Linear regressions of residue-level  $\Delta\%$ Protected values in glucose *vs*  $\Delta\%$ Protected in trehalose yield slopes and correlation coefficients near 1 and intercepts near 0 for both proteins (Figures S3 and S4 and Table S3). The same analysis shows that sorbitol yields slopes and correlation coefficients near 1 and intercepts near 0 for GB1 but not CI2 (Figures S3 and S4 and Table S3). For 1,2,3-hexanetriol the slopes, correlation coefficients, and intercepts are close to 0 for both proteins (Figures S3 and S4 and Table S3).

**Dose Response.** We performed LOVE NMR on GB1 with varying doses of trehalose, glucose, and 1,2,3-hexanetriol. In addition to the 20 g/L doses described above, we assessed doses of 2 and 40 g/L trehalose, 2 g/L glucose, and 40 g/L 1,2,3-hexanetriol. For trehalose and glucose, protection increases with increasing concentration (Figure 2 and Table S6). However, 1,2,3-hexanetriol shows no dose response.

**Water Content and Glass-Transition Temperature ( $T_g$ ).** To determine if protection is related to a sugar's ability to retain water and its ability to vitrify, we performed TGA and DSC on GB1 samples lyophilized alone or with 20 g/L sugar or sugar alcohol (Figure 3). 1,2,3-Hexanetriol is more volatile than the other additives, and it coevolved with water during TGA, so water content was not quantified. Immediately after 24 h of drying, samples possess  $\sim$ 5% water by mass, which is  $<1$  layer of water on GB1 (Figure 3A).<sup>17,43</sup> After 24 h at 43% RH ( $D_2O$ ), all samples contain similar amounts,  $\sim$ 11%, which is still  $<1$  layer (Figure 3A).<sup>17,43</sup>  $T_g$  values are disparate, ranging from 10 to 65 °C at  $t_0$  (Figure 3B). As expected,<sup>44–46</sup> the additional water in the  $t_{24}$  samples decreases  $T_g$  (Figure 3B), but sugars mitigate  $T_g$  depression (i.e.,  $T_g$ , sugar  $>$   $T_g$ , no sugar at  $t_{24}$ , Figure 3B).

**Protection and Intraprotein Hydrogen Bonds.** We counted polar contacts  $\leq$ 3.4 Å and  $>120^\circ$  as hydrogen bonds using PDB 2QMT for GB1 and PDB 2CI2 for CI2 and tallied the number of intraprotein hydrogen bonds for each residue of both proteins (Figure S5 and Tables S7 and S8). These structures and hydrogen bonds come from X-ray diffraction studies, but similar results are obtained from solution NMR studies.<sup>31,47</sup>

To probe relationships between protection and protein structure, we plotted %Protected by trehalose *vs* %Protected in the absence of an additive. The same four groupings emerge for all sugars for both GB1 and CI2 (Figures 4, S6, and S7).

In GB1, L12, E15, T17, E19, V21, A23, G41, Y45, and A48 are not protected by trehalose (Figure 4B). These residues have the fewest intramolecular H-bonds, with most possessing none and no residue possessing two or more (Figure 4C). They also tend to occupy the ends of secondary structure elements (Figure 4D). G9, K13, G14, A20, D22, A24, T25, G38, W43, T49, and K50 are  $<40\%$  protected in GB1 alone, and trehalose increases protection by  $<50\%$  (Figure 4B). Most of these residues have one or two intramolecular H-bonds (Figure 4C). This group also tends to be near the ends of the secondary structure (Figure 4D). N8, K28, Q32, Y33, A34, N35, D36, N37, V39, E42, T55, and E56 experience  $<45\%$  protection in GB1 alone, increasing to  $\sim 100\%$  in trehalose (Figure 4B). None of these residues lacks intramolecular H-bonds, most have more than two, and many reside in the  $\alpha$ -helix (Figure 4C,D). Finally, Y3, K4, L5, I6, L7, T16, T18,

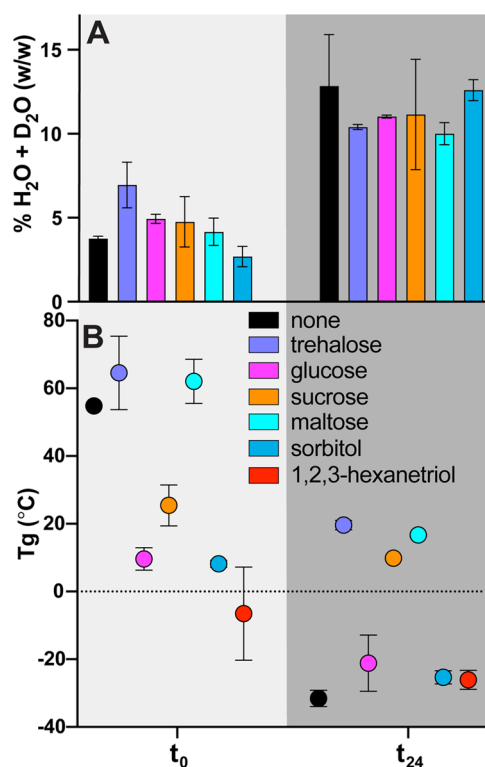


**Figure 3.** Water content and glass-transition temperature of dehydrated GB1/sugar (alcohol) mixtures before and after exposure to 43% relative  $D_2O$  humidity. Samples were lyophilized from 650  $\mu$ L of 500  $\mu$ M GB1 and 20 g/L of indicated sugar or sugar alcohol before and after ( $t_0$  and  $t_{24}$ , respectively) incubation in 43% RH  $D_2O$ . (A) Percent  $H_2O$  ( $t_0$ ) or  $H_2O + D_2O$  ( $t_{24}$ ) by weight. Error bars represent the standard deviation from six independent measurements for GB1 at  $t_0$  with trehalose, eight independent measurements with sucrose, and three independent measurements for other data. (B) Glass-transition temperature,  $T_g$ . Error bars represent the standard deviation of three independent measurements. For some measurements, uncertainties are smaller than the points.

A26, E27, V29, F30, K31, T44, D46, T51, F52, T53, and V54 are highly protected ( $>55\%$ ) in GB1 alone, and their protection increases to 100% in trehalose (Figure 4B). All global-unfolding residues<sup>30</sup> are included in this last group, all have two or more H-bonds, and all reside in structured regions (Figure 4A–D).

For CI2, the picture is similar, although the four groups are less obvious (Figure 4). E7, E26, V31, I37, T39, and Y42 are not protected by trehalose (Figure 4F). These residues have zero or one H-bond (Figure 4G) and tend to occupy less structured regions (Figure 4H). E4, S12, V13, E14, E15, K17, A27, I29, V38, and L54 are  $<40\%$  protected in CI2 alone, and trehalose increases protection by  $<50\%$  (Figure 4F). Most of these residues have zero to two intramolecular H-bonds (Figure 4G). This group also tends to occupy unstructured regions or reside near the ends of the secondary structure (Figure 4H). V9, K18, Q28, V32, G35, R43, R48, R62, V63, and G64 experience  $<40\%$  protection in CI2 alone, increasing by  $>50\%$  in trehalose (Figure 4F). These residues possess a wider range of H-bonds, and many occupy structured regions (Figure 4G,H). Finally, W5, K11, A16, V19, I20, L21, Q22, K24, I30, L32, R46, V47, L49, F50, V51, D52, N56, I57, A58, E59, and V60 are highly protected ( $>45\%$ ) in CI2 alone, increasing to  $\sim 100\%$  in trehalose (Figure 4F). All global-

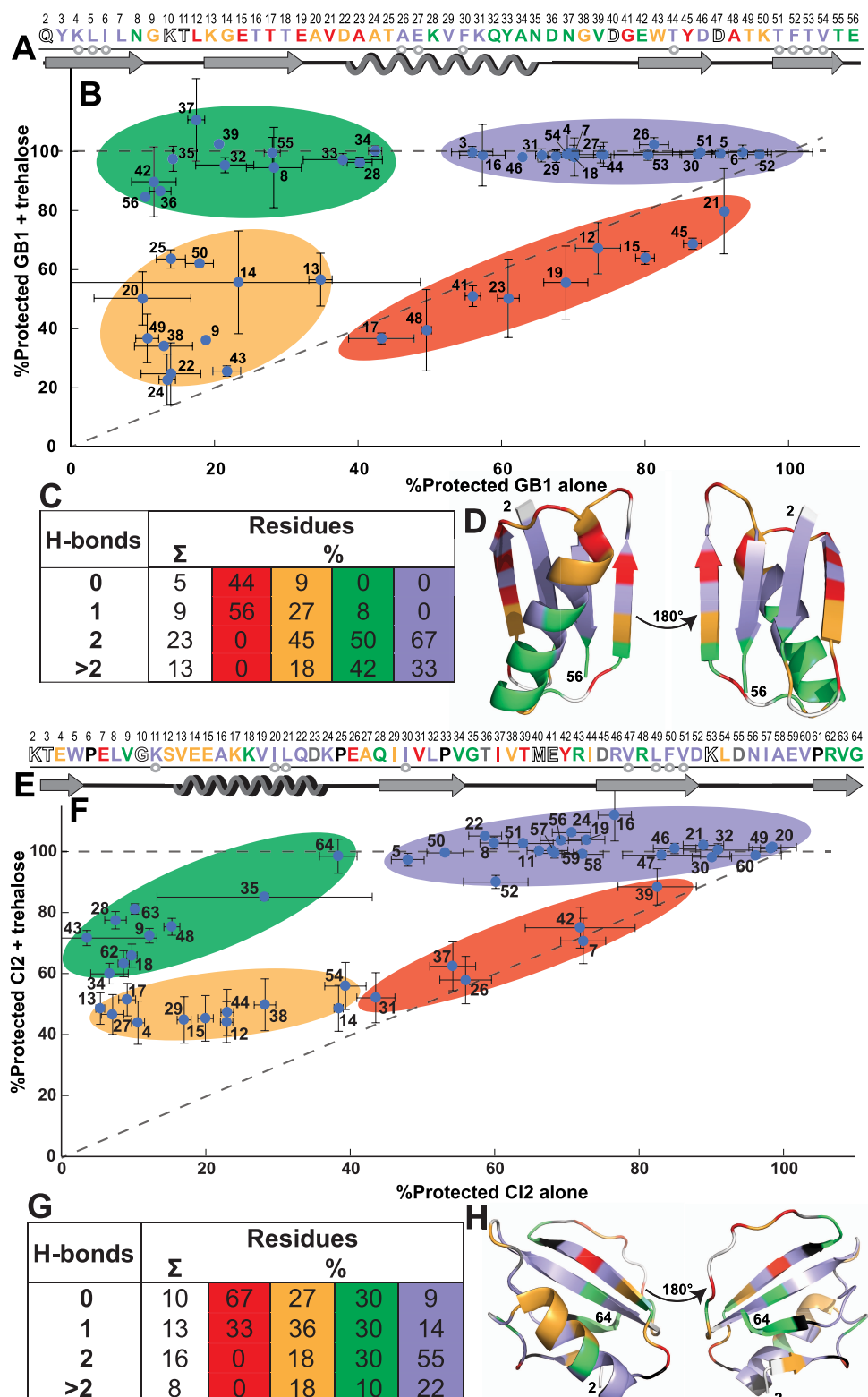


**Figure 4.** Dry-state protection of GB1 (top) and CI2 (bottom) in the presence and absence of trehalose. (A–H) Residues are color-coded by their position in panel (B) or (F). Gray circles in panels A and C indicate solution global-unfolding residues. Shaded boxes indicate missing data: open letters from rapid back exchange, gray letters from overlapping peaks, and prolines. Error bars represent standard deviations propagated from triplicate analysis. (B, F) %Protected protein + trehalose vs %Protected protein alone. Horizontal and diagonal dashed lines are of no theoretical significance. Shaded ellipses group the data (red, trehalose has little effect on protection; orange, <45 %Protected in protein alone and <50 Δ% Protected by trehalose; green, <45 %Protected in protein alone but >50 Δ%Protected by trehalose; purple, >45 %Protected in protein alone but ~100% in trehalose). (C, G) H-bonds and protection.  $\Sigma$  indicates the number of residues with LOVE NMR data with 0, 1, 2, or >2 intramolecular H-bonds from PDB 2QMT or 2CI2. Colored columns show the percent of residues from each group with 0, 1, 2, or >2 intramolecular H-bonds. (D, H) Color-coded groupings from panels B and F mapped onto the respective structures.

unfolding residues<sup>31</sup> are included in this group, and most have at least two H-bonds and occur in structured regions (Figure 4E–H).

These groups are recognizable in glucose, sucrose, fucose, and rhamnose for both proteins and in maltose for GB1 (Figures S6 and S7). In L-galactose, the pattern is recognizable in GB1, but the groups overlap more, perhaps because only one experiment was performed due to the cost of this sugar. Sorbitol also protects residues in GB1 with this pattern but not CI2 (Figures S6 and S7). In hexanetriol, this pattern is not discernible in either protein (Figures S6 and S7).

## DISCUSSION

Protection is nearly sugar-agnostic; at 20 g/L, trehalose, glucose, sucrose, maltose, fucose, and rhamnose protect the proteins similarly despite their differing structures (Figures 1, 2, S1, and S2). Despite the potential for reducing sugars to oxidize or covalently react with the proteins *via* the Maillard reaction [i.e., glycation<sup>48</sup>], nonreducing and reducing sugars behave the same here. This result is consistent with those from efforts showing that trehalose and sucrose,<sup>49</sup> glucose and sucrose,<sup>21</sup> and glucose and maltose<sup>50</sup> are similarly protective during lyophilization.

More detailed insight is gained by comparing LOVE NMR data to the structures of GB1 and CI2. To facilitate this analysis, we use colors defined by the effect of trehalose on protection (Figure 4): red, trehalose does not protect; orange, low protection that increases moderately in trehalose; green, low protection increasing to ~100%; purple, highly protected and rising to ~100% in trehalose.

We focus on trehalose, but the LOVE NMR data (Figures 1, 2, 4, S2, S3, S4, S6, and S7 and Table S3) indicate our analysis applies to all sugars (but not necessarily sugar alcohols) tested. Residues that are highly protected even in the absence of an additive and whose protection increases in trehalose (purple group) occupy structured regions and include the global-unfolding residues,<sup>30,31</sup> supporting the notion that these protectants generally safeguard native structure rather than impose a new structure. Maintaining native structure in the dry state is important for activity recovery upon rehydration.<sup>21,51,52</sup>

Residues with a greater number of intramolecular H-bonds are better protected than residues with fewer H-bonds (Figures 4, S6, and S7 and Tables S7 and S8). In fact, residues lacking intramolecular H-bonds are often not protected (red group). Solution-based efforts show that glucose and sorbitol weaken protein–solvent H-bonds while strengthening intramolecular protein H-bonds and shortening backbone H-bonds of a protein nearly identical to GB1.<sup>53</sup> Perhaps sugars have this effect on the H-bonds of proteins during drying as well. These observations and comparisons suggest that as GB1 or CI2 dries, sugars preserve structure by stabilizing native intramolecular H-bonds.

We investigated how removing hydroxyl groups influences protection. For both GB1 and CI2, taking away one hydroxyl group [fucose (deoxy-L-galactose) and rhamnose (deoxy-L-mannose)] does not decrease protection compared to other monosaccharides (glucose and L-galactose, Figure 2 and Tables S1, S2, S4, and S5). Under these conditions, if there is an effect, it is too small to observe. However, removing three hydroxyl groups (1,2,3-hexanetriol) decreases protection of both proteins (Figure 2 and Tables S4 and S5).

The loss of protection with the loss of three hydroxyl groups supports the conclusion that protection also arises by water

replacement<sup>21,22</sup> because hydroxyl groups on sugars can form H-bonds to exposed polar groups upon water loss. Most of the residues that show low protection alone but ~100% protection in trehalose are solvent-exposed; more than 80% have an H-bond-competent side chain in GB1, and 50% do in CI2 (Figure 4). Although total, backbone, or side chain solvent-accessible surface area does not correlate with differences in protection for either protein, polar solvent-accessible surface area has a positive, weak, but significant correlation for both proteins (Figure S9). These data support the idea that sugars replace H-bonds provided by water in solution. The residual protection by 1,2,3-hexanetriol may arise from the remaining hydroxyl groups and from simple occlusion by the additive, but as discussed below, the presence of the exposed hydrophobic groups could decrease protection.

Sorbitol protects CI2 less well than glucose but protects GB1 equally well, indicating that linearizing a monosaccharide can decrease protection (Figure 2 and Tables S1, S2, S4, and S5). Sorbitol protects GB1 more like sugars with respect to the impact of intramolecular hydrogen bonding than CI2 (Figures S6 and S7). Other efforts support this protein-specific effect; sorbitol can protect a lyophilized protein comparably to maltose,<sup>50</sup> sucrose, and glucose,<sup>54</sup> or worse than sucrose and trehalose.<sup>49</sup> GB1 and CI2 are similar in size but not in secondary structure, and, at the pH used here (6.5), GB1 is more charged (−4.0) than CI2 (−0.9). LOVE NMR data show that disordered proteins protect CI2 less than GB1, and the globular protein bovine serum albumin is ineffective for both proteins.<sup>26</sup> Here, both proteins are protected similarly by every sugar and sugar alcohol except sorbitol (Figure 2). We note that linear sorbitol is more flexible than ring-forming sugars, and disordered proteins are more flexible than globular proteins. Perhaps flexibility-enhanced polar interactions involving sorbitol and flexibility-enhanced electrostatic interactions of disordered proteins permit more effective H-bond protection.

We examined residues that are at least 20% less protected in the sugar alcohols sorbitol and 1,2,3-hexanetriol than they are in the sugar trehalose (Figure S8). For GB1, these residues are N8, T16, and D36 in sorbitol and N8, T16, A20, T25, K28, Q32, Y33, A34, N35, D36, V39, E42, K50, T55, and E56 in 1,2,3-hexanetriol. In CI2, these residues are E4, W5, L8, V9, V13, K17, K18, A27, Q28, I29, V34, R43, I44, R62, and V63 in sorbitol and E4, W5, V9, V13, K17, K18, Q22, A27, Q28, I29, V34, R43, R48, R62, and V63 in 1,2,3-hexanetriol. For GB1, all of these residues except V39 have at least two intramolecular H-bonds, and for CI2, all of these residues have at least one intramolecular H-bond except E4, I29, G35, R48, and R62. This observation supports the idea that sugar alcohols do a worse job of stabilizing intramolecular H-bonds than sugars. None of these residues are in the red group (no protection by trehalose); the unprotected residues are not further deprotected by sugar alcohols. We also observe that intramolecular H-bonds do not contribute to protection in 1,2,3-hexanetriol, unlike the sugars (Figures S6 and S7). Furthermore, 1,2,3-hexanetriol does not provide a dose response to protection like trehalose and glucose (Figure 2). Perhaps the three-carbon chain on the end of 1,2,3-hexanetriol interacts with hydrophobic residues and pulls apart the protein as it dries (Figure S1).

If these sugars protect GB1 by water retention, GB1/sugar mixtures would have higher water contents than GB1 alone. Instead, the TGA data show that GB1/sugar samples and GB1

alone have similar water contents at  $t_0$  despite the protective effects of sugars (Figure 3A). The same holds at  $t_{24}$ . Our observation suggests that sugars do not protect via water retention, in agreement with other reports.<sup>54</sup> For the  $t_0$  samples,  $T_g$  values cover a broad range, without a pattern that clearly corresponds to protection. While 1,2,3-hexanetriol depresses  $T_g$  most and is least protective, glucose, sucrose, and sorbitol also depress  $T_g$  compared to GB1 alone (Figure 3B) yet protect about the same as trehalose. At  $t_{24}$ , the disaccharides dramatically mitigate the plasticizing effects of water compared to GB1 alone, while glucose and the sugar alcohols slightly do (Figure 3B). These sugars, especially the disaccharides, may protect via vitrification during humid storage.

Given that all sugars tested are almost equally protective, why does nature lean so heavily on trehalose? It has been known for decades that trehalose is extraordinarily stable, being much more resistant than other sugars to hydrolysis and nonenzymatic browning.<sup>55–57</sup> For instance, the activation energy for acid hydrolysis of trehalose is 40 kcal/mol, higher than that of sucrose (25 kcal/mol) and maltose (30 kcal/mol).<sup>55</sup> The stability of all three disaccharides with  $\alpha$ -1-glycosidic linkages can be largely ascribed to the anomeric effect,<sup>58</sup> the tendency of the anomeric substituent (the oxygen on the carbon next to the pyranose oxygen) to occupy the axial rather than the sterically less hindered equatorial position. Although the physical basis of the anomeric effect remains unsettled, it is generally agreed that the added hydrolytic stability arises from the increase in energy required to access a half-chair oxocarbenium-ion transition state.<sup>58</sup>

Sugars like sucrose and maltose have one  $\alpha$ -glycosidic bond. Trehalose is unusual because it contains a symmetric, 1,1-linkage between two anomeric centers (Figure S1). This atypical glycosidic bond is simultaneously stabilized by two anomeric effects, one from each of the contributing centers. Trehalose is thus twice stabilized. Given this information, we suggest that nature selected trehalose for its high covalent stability. Several efforts report that trehalose outperforms the other sugars studied here in protecting proteins from desiccation stress.<sup>18,59–61</sup> However, in other studies, sucrose protects dry proteins similarly or even slightly better than trehalose.<sup>49,52</sup> In another report, trehalose, sucrose, and sorbitol protect differently during one drying method but the same after another drying method.<sup>62</sup> These differing observations are a reminder that protection can be client protein- and condition-dependent.

In summary, residue-level protection by sugars correlates with the number of intramolecular protein H-bonds, polar solvent accessible surface area, and H-bond-competent side chains, providing evidence that stabilizing intraprotein H-bonds and water replacement play roles in protection. The mitigating effect of sugars on  $T_g$  depression suggests a role for vitrification. However, the fact that all samples retain similar amounts of water is evidence against the water retention hypothesis. Further efforts will determine the chemical attributes necessary for the protective activity of sugars.

## ASSOCIATED CONTENT

### Supporting Information

The Supporting Information is available free of charge at <https://pubs.acs.org/doi/10.1021/acs.biochem.2c00692>.

Sugar structures; %Protected values for GB1 and CI2 in the presence and absence of cosolutes, correlation plots and coefficients for trehalose and other protectants, and intraprotein hydrogen bond counts (PDF)

### Accession Codes

GB1: UniProt P19909

CI2: UniProt P01053

## AUTHOR INFORMATION

### Corresponding Author

Gary J. Pielak – Department of Chemistry, University of North Carolina at Chapel Hill (UNC-CH), Chapel Hill, North Carolina 27599-3290, United States; Department of Biochemistry & Biophysics and Lineberger Cancer Center, UNC-CH, Chapel Hill, North Carolina 27599, United States; Integrative Program for Biological and Genome Sciences, UNC-CH, Chapel Hill, North Carolina 27599-7100, United States; [orcid.org/0000-0001-6307-542X](https://orcid.org/0000-0001-6307-542X); Phone: (919) 962-4495; Email: [gary\\_pielak@unc.edu](mailto:gary_pielak@unc.edu)

### Authors

Julia A. Brom – Department of Chemistry, University of North Carolina at Chapel Hill (UNC-CH), Chapel Hill, North Carolina 27599-3290, United States

Ruta G. Petrikis – Department of Chemistry, University of North Carolina at Chapel Hill (UNC-CH), Chapel Hill, North Carolina 27599-3290, United States

Complete contact information is available at: <https://pubs.acs.org/10.1021/acs.biochem.2c00692>

### Notes

The authors declare no competing financial interest.

## ACKNOWLEDGMENTS

This research was supported by NIH grant R01GM127291 and NSF grant CHE-2203505 to G.J.P. The authors thank Stu Parnham from the UNC Biomolecular NMR Core Laboratory and Brandie Ehrmann from the UNC Chemistry Mass Spectrometry Core Laboratory for equipment maintenance and advice. The Cores are supported by NIH grant NCI P30CA016086 and NSF grant CHE-1726291, respectively. The authors thank Elizabeth Pielak for comments on the manuscript, the Pielak lab for helpful discussion, and Albert A. Bowers and Bo Li for helping them understand the anomeric effect.

## REFERENCES

- Devi, S. Cold comfort: Getting insulin to those who need it. *Lancet* **2021**, *398*, No. 1791.
- Hill, A. B.; Kilgore, C.; McGlynn, M.; Jones, C. H. Improving global vaccine accessibility. *Curr. Opin. Biotechnol.* **2016**, *42*, 67–73.
- Morrow, T.; Felcone, L. H. Defining the difference: What makes biologics unique. *Biotechnol. Healthcare* **2004**, *1*, 24–29.
- Frokjaer, S.; Otzen, D. E. Protein drug stability: A formulation challenge. *Nat. Rev. Drug Discovery* **2005**, *4*, 298–306.
- Chang, L. L.; Pikal, M. J. Mechanisms of protein stabilization in the solid state. *J. Pharm. Sci.* **2009**, *98*, 2886–2908.
- Wang, W. Lyophilization and development of solid protein pharmaceuticals. *Int. J. Pharm.* **2000**, *203*, 1–60.
- Walters, R. H.; Bhatnagar, B.; Tchessalov, S.; Izutsu, K. I.; Tsumoto, K.; Ohtake, S. Next generation drying technologies for pharmaceutical applications. *J. Pharm. Sci.* **2014**, *103*, 2673–2695.
- Bjelošević, M.; Pobirk, A. Z.; Planinsek, O.; Grabnar, P. A. Excipients in freeze-dried biopharmaceuticals: Contributions toward

formulation stability and lyophilisation cycle optimisation. *Int. J. Pharm.* **2020**, *576*, No. 119029.

(9) Piszkiewicz, S.; Pielak, G. J. Protecting enzymes from stress-induced inactivation. *Biochemistry* **2019**, *58*, 3825–3833.

(10) Ohtake, S.; Kita, Y.; Arakawa, T. Interactions of formulation excipients with proteins in solution and in the dried state. *Adv. Drug Delivery Rev.* **2011**, *63*, 1053–1073.

(11) Jain, N. K.; Roy, I. Effect of trehalose on protein structure. *Protein Sci.* **2009**, *18*, 24–36.

(12) Richards, A. B.; Krakowka, S.; Dexter, L. B.; Schmid, H.; Wolterbeek, A. P. M.; Waalkens-Berendsen, D. H.; Shigoyuki, A.; Kurimoto, M. Trehalose: A review of properties, history of use and human tolerance, and results of multiple safety studies. *Food Chem. Toxicol.* **2002**, *40*, 871–898.

(13) Hengherr, S.; Heyer, A. G.; Kohler, H. R.; Schill, R. O. Trehalose and anhydrobiosis in tardigrades - evidence for divergence in responses to dehydration. *FEBS J.* **2008**, *275*, 281–288.

(14) Elbein, A. D.; Pan, Y. T.; Pastuszak, I.; Carroll, D. New insights on trehalose: A multifunctional molecule. *Glycobiology* **2003**, *13*, 17R–27R.

(15) Boothby, T. C.; Pielak, G. J. Intrinsically disordered proteins and desiccation tolerance: Elucidating functional and mechanistic underpinnings of anhydrobiosis. *BioEssays* **2017**, *39*, No. 1700119.

(16) Xie, G.; Timashoff, S. N. The thermodynamic mechanism of protein stabilization by trehalose. *Biophys. Chem.* **1997**, *64*, 25–43.

(17) Crilly, C. J.; Brom, J. A.; Kowalewski, M. E.; Piszkiewicz, S.; Pielak, G. J. Dried protein structure revealed at the residue level by liquid-observed vapor exchange NMR. *Biochemistry* **2021**, *60*, 152–159.

(18) Colaço, C.; Sen, S.; Thangavelu, M.; Pinder, S.; Roser, B. Extraordinary stability of enzymes dried in trehalose: Simplified molecular biology. *Bio/Technology* **1992**, *10*, 1007–1011.

(19) Mensink, M. A.; Frijlink, H. W.; van der Voort Maarschalk, K.; Hinrichs, W. L. How sugars protect proteins in the solid state and during drying (review): Mechanisms of stabilization in relation to stress conditions. *Eur. J. Pharm. Biopharm.* **2017**, *114*, 288–295.

(20) Lerbret, A.; Affouard, F.; Hedoux, A.; Krenzlin, S.; Siepmann, J.; Bellissent-Funel, M. C.; Descamps, M. How strongly does trehalose interact with lysozyme in the solid state? Insights from molecular dynamics simulation and inelastic neutron scattering. *J. Phys. Chem. B* **2012**, *116*, 11103–11116.

(21) Prestrelski, S. J.; Tedeschi, N.; Arakawa, T.; Carpenter, J. F. Dehydration-induced conformational transitions in proteins and their inhibition by stabilizers. *Biophys. J.* **1993**, *65*, 661–671.

(22) Carpenter, J. F.; Crowe, J. H. An infrared spectroscopic study of the interactions of carbohydrates with dried proteins. *Biochemistry* **1989**, *28*, 3916–3922.

(23) Di Gioacchino, M.; Bruni, F.; Ricci, M. A. Protection against dehydration: A neutron diffraction study on aqueous solutions of a model peptide and trehalose. *J. Phys. Chem. B* **2018**, *122*, 10291–10295.

(24) Grasmeijer, N.; Stankovic, M.; de Waard, H.; Frijlink, H. W.; Hinrichs, W. L. J. Unraveling protein stabilization mechanisms: Vitrification and water replacement in a glass transition temperature controlled system. *Biochim. Biophys. Acta, Proteins Proteomics* **2013**, *1834*, 763–769.

(25) Crilly, C.; Eicher, J. E.; Warmuth, O.; Atkin, J. M.; Pielak, G. J. Water's variable role in protein stability uncovered by liquid-observed vapor exchange NMR. *Biochemistry* **2021**, *60*, 3041–3045.

(26) Crilly, C. J.; Brom, J. A.; Warmuth, O.; Esterly, H. J.; Pielak, G. J. Protection by desiccation-tolerance proteins probed at the residue level. *Protein Sci.* **2022**, *31*, 396–406.

(27) Englander, S. W.; Kallenbach, N. R. Hydrogen exchange and structural dynamics of proteins and nucleic acids. *Q. Rev. Biophys.* **1983**, *16*, 521–655.

(28) Desai, U. R.; Osterhout, J. J.; Klibanov, A. M. Protein structure in the lyophilized state: A hydrogen isotope exchange/NMR study with bovine pancreatic trypsin inhibitor. *J. Am. Chem. Soc.* **1994**, *116*, 9420–9422.

(29) Percy, A. J.; Rey, M.; Burns, K. M.; Schriemer, D. C. Probing protein interactions with hydrogen/deuterium exchange and mass spectrometry-A review. *Anal. Chim. Acta* **2012**, *721*, 7–21.

(30) Orban, J.; Alexander, P.; Bryan, P.; Khare, D. Assessment of stability differences in the protein G B1 and B2 domains from hydrogen-deuterium exchange: Comparison with calorimetric data. *Biochemistry* **1995**, *34*, 15291–15300.

(31) Itzhaki, L. S.; Neira, J. L.; Fersht, A. R. Hydrogen exchange in chymotrypsin inhibitor 2 probed by denaturants and temperature. *J. Mol. Biol.* **1997**, *270*, 89–98.

(32) Glasoe, P. K.; Long, F. A. Use of glass electrodes to measure acidities in deuterium oxide. *J. Phys. Chem. A* **1960**, *64*, 188–190.

(33) Charlton, L. M.; Barnes, C. O.; Li, C.; Orans, J.; Young, G. B.; Pielak, G. J. Residue-level interrogation of macromolecular crowding effects on protein stability. *J. Am. Chem. Soc.* **2008**, *130*, 6826–6830.

(34) Greenspan, L. Humidity fixed points of binary saturated aqueous solutions. *J. Res. Natl. Bur. Stand., Sect. A* **1977**, *81A*, 89–96.

(35) Sophocleous, A. M.; Zhang, J.; Topp, E. M. Localized hydration in lyophilized myoglobin by hydrogen-deuterium exchange mass spectrometry. 1. Exchange mapping. *Mol. Pharmaceutics* **2012**, *9*, 718–726.

(36) May, J. C.; Grim, E.; Wheeler, R. M.; West, J. Determination of residual moisture in freeze-dried viral vaccines: Karl Fischer, gravimetric and thermogravimetric methodologies. *J. Biol. Stand.* **1982**, *10*, 249–259.

(37) May, J. C.; Wheeler, R. M.; Grim, E. The gravimetric method for the determination of residual moisture in freeze-dried biological products. *Cryobiology* **1989**, *26*, 277–284.

(38) Aguilera, J. M.; Levi, G.; Karel, M. Effect of water content on the glass transition and caking of fish protein hydrolysates. *Biotechnol. Prog.* **1993**, *9*, 651–654.

(39) Kalichevsky, M. T.; Jaroszkiewicz, E. M.; Blanshard, J. M. V. Glass transition of gluten. 1: Gluten and gluten-sugar mixtures. *Int. J. Biol. Macromol.* **1992**, *14*, 257–266.

(40) Sochava, I. V.; Smirnova, O. I. Heat capacity of hydrated and dehydrated globular proteins. Denaturation increment of heat capacity. *Food Hydrocolloids* **1993**, *6*, 513–524.

(41) Noel, T. R.; Parker, R.; Ring, S. G.; Tatham, A. S. The glass-transition behaviour of wheat gluten proteins. *Int. J. Biol. Macromol.* **1995**, *17*, 81–85.

(42) Duddu, S. P.; Dal Monte, P. R. Effect of glass transition temperature on the stability of lyophilized formulations containing a chimeric therapeutic monoclonal antibody. *Pharm. Res.* **1997**, *14*, 591–595.

(43) Brom, J. A.; Pielak, G. J. Desiccation-tolerance and globular proteins adsorb similar amounts of water. *Protein Sci.* **2022**, *31*, No. e4288.

(44) Haque, M. K.; Roos, Y. H. Water sorption and plasticization behavior of spray-dried lactose/protein mixtures. *J. Food Sci.* **2004**, *69*, 384–391.

(45) Pikal, M. J.; Rigsbee, D. R.; Roy, M. L. Solid state chemistry of proteins: I. Glass transition behavior in freeze dried disaccharide formulations of human growth hormone (hGH). *J. Pharm. Sci.* **2007**, *96*, 2765–2776.

(46) Grunina, N. A.; Belopolskaya, T. V.; Tsereteli, G. I. The glass transition process in humid biopolymers. DSC study. *J. Phys.: Conf. Ser.* **2006**, *40*, 105–110.

(47) Gronenborn, A. M.; Filpula, D. R.; Essig, N. Z.; Achari, A.; Whitlow, M.; Wingfield, P. T.; Clore, G. M. A novel, highly stable fold of the immunoglobulin binding domain of streptococcal protein G. *Science* **1991**, *253*, 657–661.

(48) Wautier, J. L.; Schmidt, A. M. Protein glycation: A firm link to endothelial cell dysfunction. *Circ. Res.* **2004**, *95*, 233–238.

(49) Kadoya, S.; Fujii, K.; Izutsu, K.; Yonemochi, E.; Terada, K.; Yomota, C.; Kawanishi, T. Freeze-drying of proteins with glass-forming oligosaccharide-derived sugar alcohols. *Int. J. Pharm.* **2010**, *389*, 107–113.

(50) Tanaka, K.; Takeda, T.; Miyajima, K. Cryoprotective effect of saccharides on denaturation of catalase by freeze-drying. *Chem. Pharm. Bull.* **1991**, *39*, 1091–1094.

(51) Dong, A.; Prestrelski, S. J.; Allison, S. D.; Carpenter, J. F. Infrared spectroscopic studies of lyophilization- and temperature-induced protein aggregation. *J. Pharm. Sci.* **1995**, *84*, 415–424.

(52) Chang, L. L.; Shepherd, D.; Sun, J.; Ouellette, D.; Grant, K. L.; Tang, X. C.; Pikal, M. J. Mechanism of protein stabilization by sugars during freeze-drying and storage: Native structure preservation, specific interaction, and/or immobilization in a glassy matrix? *J. Pharm. Sci.* **2005**, *94*, 1427–1444.

(53) Li, J.; Chen, J.; An, L.; Yuan, X.; Yao, L. Polyol and sugar osmolytes can shorten protein hydrogen bonds to modulate function. *Commun. Biol.* **2020**, *3*, No. 528.

(54) Hellman, K.; Miller, D. S.; Cammack, K. A. The effect of freeze-drying on the quaternary structure of L-asparaginase from *Erwinia carotovora*. *Biochim. Biophys. Acta, Protein Struct. Mol. Enzymol.* **1983**, *749*, 133–142.

(55) Bemiller, J. N. Acid-Catalyzed Hydrolysis of Glycosides. In *Advances in Carbohydrate Chemistry*; Elsevier, 1967; Vol. 22, pp 25–108.

(56) Schebor, C.; Burin, L.; del Pilar Buera, M.; Chirife, J. Stability to hydrolysis and browning of trehalose, sucrose and raffinose in low-moisture systems in relation to their use as protectants of dry biomaterials. *LWT-Food Sci. Technol.* **1999**, *32*, 481–485.

(57) Colaco, C. A. L. S.; Smith, C. J. S.; Sen, S.; Roser, D. H.; Newman, Y.; Ring, S.; Roser, B. J. Chemistry of Protein Stabilization by Trehalose. In *ACS Symposium Series*; Cleland, J. L.; Langer, R., Eds.; American Chemical Society, 1994; pp 222–240.

(58) Edward, J. T. Anomeric Effect. In *The Anomeric Effect and Associated Stereoelectronic Effects*; Thatcher, G. R. J., Ed.; American Chemical Society, 1993; pp 1–5.

(59) Chang, B. S.; Reeder, G.; Carpenter, J. F. Development of a stable freeze-dried formulation of recombinant human interleukin-1 receptor antagonist. *Pharm. Res.* **1996**, *13*, 243–249.

(60) Lopez-Diez, E. C.; Bone, S. The interaction of trypsin with trehalose: An investigation of protein preservation mechanisms. *Biochim. Biophys. Acta, Gen. Subj.* **2004**, *1673*, 139–148.

(61) Sun, W. Q.; Davidson, P. Protein inactivation in amorphous sucrose and trehalose matrices: Effects of phase separation and crystallization. *Biochim. Biophys. Acta, Gen. Subj.* **1998**, *1425*, 235–244.

(62) Liao, Y.-H.; Brown, M. B.; Quader, A.; Martin, G. P. Protective mechanism of stabilizing excipients against dehydration in the freeze-drying of proteins. *Pharm. Res.* **2002**, *19*, 1854–1861.

## □ Recommended by ACS

### Gut Bacteria Involved in Ellagic Acid Metabolism To Yield Human Urolithin Metabotypes Revealed

Carlos E. Iglesias-Aguirre, María V. Selma, *et al.*

FEBRUARY 25, 2023

JOURNAL OF AGRICULTURAL AND FOOD CHEMISTRY

READ 

### Discovery and Mechanistic Analysis of Structurally Diverse Inhibitors of Acetyltransferase EIs among FDA-Approved Drugs

Allan H. Pang, Oleg V. Tsodikov, *et al.*

JANUARY 19, 2023

BIOCHEMISTRY

READ 

### Biotin Binding Hardly Affects Electron Transport Efficiency across Streptavidin Solid-State Junctions

Sudipta Bera, David Cahen, *et al.*

JANUARY 17, 2023

LANGMUIR

READ 

### Rapid Estimation of Climate–Air Quality Interactions in Integrated Assessment Using a Response Surface Model

Sebastian D. Eastham, Noelle E. Selin, *et al.*

FEBRUARY 14, 2023

ACS ENVIRONMENTAL AU

READ 

Get More Suggestions >